European Radiology (2019) 29:6971–6981
https://doi.org/10.1007/s00330-019-06308-3

UROGENITAL

Diagnosing adenomyosis with MRI: a prospective study revisiting the junctional zone thickness cutoff of 12 mm as a diagnostic marker

Tina Tellum[1,2,3] · Gordana V. Matic[1,3] · Johann B. Dormagen[1,3] · Staale Nygaard[4] · Ellen Viktil[1,3] · Erik Qvigstad[1,2,3] · Marit Lieng[1,2,3]

Received: 12 October 2018 / Revised: 5 May 2019 / Accepted: 5 June 2019 / Published online: 1 July 2019

Abstract

Objectives To assess the diagnostic accuracy of a junctional zone (JZ) thickness of ≥ 12 mm and morphological features of the JZ in MRI in diagnosing adenomyosis in a premenopausal study population.

Methods This single-center, prospective observational study consecutively enrolled 93 premenopausal women suffering from a benign gynecological condition, from September 2014 to August 2016. Institutional review board approval and written consent were obtained. All participants underwent MRI and hysterectomy with a histopathological examination. MR images were evaluated in a blinded fashion by two independent readers. The maximum junctional zone thickness (JZ_{max}), presence of $JZ_{max} \geq 12$ mm, and any irregular appearance of the JZ (defined as irregular outer or inner borders, focal thickening, presence of high-intensity signal foci, or fingerlike indentations at the inner border) were documented, and the diagnostic performance was evaluated with the AUC, chi-square test, and multiple regression.

Results Adenomyosis was histopathologically confirmed in 57 (61%) of the women. JZ_{max} was not positively correlated with adenomyosis diagnosis (AUC = 0.57, $p = 0.26$) and did not differ significantly between those with and without adenomyosis (10.3 vs 10.1 mm, $p = 0.88$), nor was a cutoff of $JZ_{max} \geq 12$ mm ($n = 30/57$ (53%) vs $n = 16/36$ (44%), $p = 0.29$). The presence of an irregular JZ showed the best association with adenomyosis among the evaluated signs (sensitivity 74% (95% CI, 60, 85); specificity 83% (95% CI, 67, 94) ($p < 0.001$)).

Conclusions JZ_{max} was not correlated with adenomyosis in the present premenopausal study population, but direct signs of adenomyosis such as irregularities of the JZ provided a good diagnostic accuracy.

Key Points

- *Measuring the junctional zone thickness is of limited value for diagnosing adenomyosis with MRI and should not be used for diagnosing adenomyosis in premenopausal women with moderate disease severity.*
- *An irregular appearance of the junctional zone, the presence of myometrial cysts, and adenomyoma appear to provide the highest specificity for diagnosing adenomyosis.*
- *A consensus for the definition and reading of the junctional zone is needed.*

Keywords Adenomyosis · Magnetic resonance imaging · Hysterectomy · Prospective studies · Infertility

Electronic supplementary material The online version of this article (https://doi.org/10.1007/s00330-019-06308-3) contains supplementary material, which is available to authorized users.

✉ Tina Tellum
tina.tellum@gmail.com

[1] Department of Gynecology, Oslo University Hospital, PB 4950, Nydalen, N-0424 Oslo, Norway

[2] Institute of Clinical Medicine, Faculty of Medicine, University of Oslo, Oslo, Norway

[3] Department of Radiology and Nuclear Medicine, Oslo University Hospital, Oslo, Norway

[4] Department of Informatics, The Faculty of Mathematics and Natural Sciences, University of Oslo, Oslo, Norway

Abbreviations

AUC	Area under the receiver operating characteristics curve
ICC	Intraclass correlation coefficient
JZ	Junctional zone
MRI	Magnetic resonance imaging
NPV	Negative predictive value
PPV	Positive predictive value
R1	Reader 1
R2	Reader 2
ROC	Receiver operating characteristics
T1W	T1-weighted
T2W	T2-weighted
TSE	Turbo spin echo

Introduction

Adenomyosis is a common condition whose prevalence is described to be about 20% among women attending a general gynecological clinic [1]. It is defined by the presence of ectopic endometrial tissue located in the muscular wall of the uterus [2]. The predominant symptoms of adenomyosis are severe dysmenorrhea and heavy menstrual bleeding, which cause concomitant diseases such as anemia and reduce the quality of life [3, 4]. Several recent studies show also wider implications of this condition, such as a negative impact on fertility and pregnancy outcome, with, for example, an elevated risk for miscarriage, preeclampsia, and having a small for gestational age child [5, 6]. Therefore, it has become a greater interest to identify younger, fertile women that have adenomyosis. Magnetic resonance imaging (MRI) and transvaginal ultrasound play the most important roles in diagnosing adenomyosis [7]. Various imaging features of adenomyosis have been described, such as increased thickness of the junctional zone (JZ), ill-defined areas of low signal intensity, or bright foci on T2-weighted images, which represent foci of heterotopic endometrial tissue [8]. A cutoff of ≥ 12 mm for the JZ thickness has been previously described as a key marker of adenomyosis [9–11]. Although adenomyosis is a frequent clinical challenge, only three studies have investigated the diagnostic accuracy of MRI compared with the gold standard which is histopathology; those studies were performed 18–23 years ago [9–11]. A large proportion of the women included in those studies were elder or postmenopausal, and it is questionable if the diagnostic accuracy of the obtained diagnostic parameters can be transferred to younger women. Over the last decades, there has been a continuous evolvement of MRI techniques on the female pelvis resulting in faster acquisition with fewer artifacts and higher image resolution. The main objective of the present study was therefore to prospectively determine the diagnostic accuracy of the JZ thickness in a premenopausal study population, along with other diagnostic markers as secondary objectives, using MRI.

Material and methods

This prospective observational study was approved by the institutional review board and the regional committee for medical research ethics (approval number 2014/637) and is registered at www.clinicaltrials.gov (registration number NCT02201719). All study participants provided written consent prior to their inclusion.

Study participants

Women that were referred to the Department of Gynecology due to a benign condition requiring hysterectomy (symptomatic fibroids, heavy menstrual bleeding, pain, or a combination of these) were consecutively enrolled in the study. All women were examined clinically for inclusion by the first investigator (T.T.) from September 2014 to August 2016 and a transvaginal ultrasound was performed. The results of the ultrasound examination are reported elsewhere [12]. Inclusion criteria were being aged 30–50 years, having a benign condition, and hysterectomy being recommended as the appropriate treatment by a gynecologist. Exclusion criteria were the presence of malignancy, the use of any hormonal medication 3 months prior to the ultrasound examination and hysterectomy, or the need to morcellate the uterus during the hysterectomy. Figure 1 shows the study flowchart. The baseline characteristics did not differ significantly between the two study groups, except for the mean age being higher in the group with adenomyosis (Table 1). The indications for hysterectomy were the following for women with and without adenomyosis, and more than one indication was often present at the same time: chronic pelvic pain 25 (44%) and 16 (44%), dysmenorrhea 46 (81%) and 22 (61%), bulk-related symptoms 8 (14%) and 16 (50%), and heavy menstrual bleeding 46 (81%) and 23 (64%). "Other therapy" included a levonorgestrel intrauterine device ($n = 21$), embolization ($n = 2$), or a need for laparoscopic subtotal hysterectomy with morcellation ($n = 2$). The main exclusion criteria were the use of hormone therapy, wanting laparoscopic subtotal hysterectomy, or not wanting any therapy.

Magnetic resonance imaging

MRI was performed with a 3-Tesla (T) Philips Ingenia with dStream anterior and posterior coils, or 1.5-T Philips Achiva device with a 32-channel cardiac coil (Philips Medical Systems). On the 3.0-T system, T2-weighted (T2W) turbo spin echo (TSE) images were acquired in the sagittal plane, oblique axial plane perpendicular to the long axis of the uterine cavity, and oblique coronal plane parallel to the long axis of the uterine cavity. T1-weighted (T1W) TSE and T1W fat-

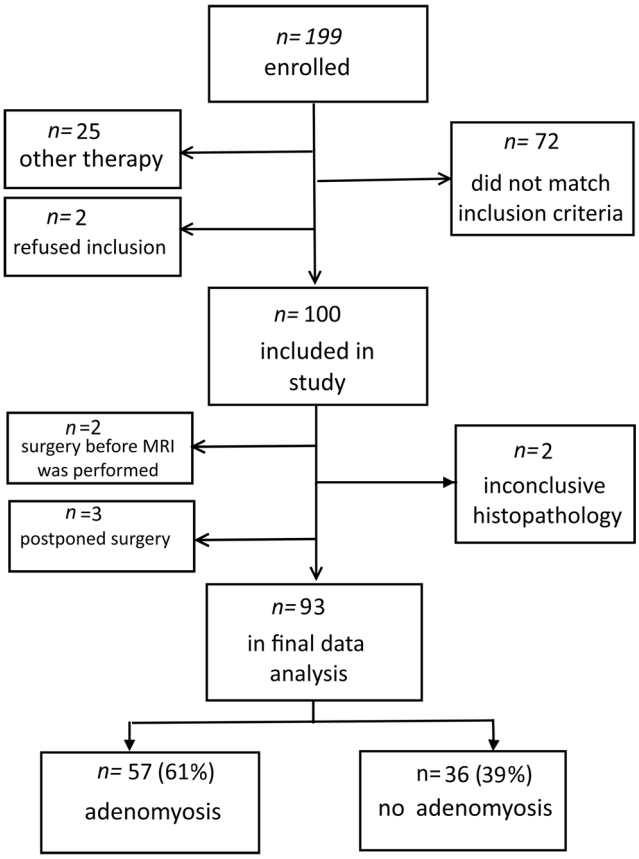

Fig. 1 Study flowchart. MRI, magnetic resonance imaging

suppressed images were acquired in the oblique axial plane. On the 1.5-T system, 3D balanced turbo field echo and 3D T2W were acquired in the axial plane with sagittal and coronal reformates, T1W TSE with and without fat suppression, and T2W TSE in the oblique axial plane. The acquisition parameters are provided in Supplementary Table 1 (online). Examinations were performed regardless of the menstrual cycle phase. Patient preparation included fasting for 4 h before the examination, voiding of the bladder, and administration of 20 mg of butylscopolamine (Buscopan, Sanofi-aventis) intravenously and 1 mg of glucagon intramuscularly. In seven cases, the MRI had already been performed at another institution and the acquired images were retrieved and reassessed. When the quality was not satisfying, the MRI was performed again (two cases). The median time interval between the MRI was performed and the surgery was 41 days (range, 1–308 days).

Image interpretation

All images were stored anonymously on the Syngo Imaging picture archiving and communication system (Siemens Healthcare). G.M. (reader 1, R1), with 14 years of body MRI experience and who was blinded for both the sonographic and histopathological data, performed the reading of all images. All evaluated features are listed and defined in Table 2. We defined adenomyosis as being present if one or more of $JZ_{max} \geq 12$ mm, myometrial cysts, or adenomyoma which are comprehensively described elsewhere were present [9, 10, 13–16]. Other features that have been described less comprehensively previously were also documented and tested for their diagnostic accuracy [10, 11, 17]. One of the less-described features is the morphological classification of the JZ that is introduced here. It is based on previously described features and modified for MRI (Fig. 2) [10, 18]. There is no unanimous definition of the JZ in MRI and it is measured in different ways among radiologists and research groups. In order to reflect that variation, we therefore introduce different terms of JZ measurements (JZ_{max} and $JZ_{max\text{-}A}$) that reflect different measurement practices that we used in our clinical work and found in the literature [8, 19, 20]. Those are comprehensively explained in Table 2 and Fig. 3. R1 repeated the reading of the predictors JZ_{max}, JZ_{min}, and JZ_{diff} 6 months after the first reading, to enable testing of the intra-reader agreement of those signs and confirm the reliability of the results. A second reader (E.V., here R2, with 20 years of body

Table 1 Baseline characteristics of the study population

	Adenomyosis, $n = 57$	No adenomyosis, $n = 36$	p
Age, years	43.5 ± 4.9	41.2 ± 4.2	0.01*
Body mass index, kg/m^2	25.9 (16–44)	25.6 (19–34)	0.73
Parity	1.4 ± 1.4	1.5 ± 1.2	0.66
Presence of fibroids	33 (58%)	18 (50%)	0.46
Presence of fibroids > 50 mm	4 (7%)	10 (27%)	0.03*
Number of histopathological sections obtained from the corpus uteri	8.6 ± 2.5	8.6 ± 2.7	0.68

Adenomyosis/no adenomyosis confirmed by histopathology. Data are mean ± standard deviation, n (%), or median (range) values. *p was determined using Student's t test or the Mann-Whitney U test; a value ≤ 0.05 was considered statistically significant

Table 2 Definition of predictors for the diagnosis of adenomyosis and other documented features

	Definition
Signs used for diagnosing adenomyosis	
$JZ_{max} \geq 12$ mm [a]	JZ is a low-intensity band in T2W MRI of the inner myometrium, lining the endometrial cavity. JZ ≥ 12 mm, measured in any plane, including focal enlargement, and not including adjacent focal adenomyoma (definition see below) or diffuse adenomyosis[b]
Myometrial cysts	High-intensity foci in the myometrium or subendometrial area, as seen in T2W or T1W imaging (hemorrhagic content)
Adenomyoma	Ill-defined focal, low-intensity areas with or without high-intensity foci
Other documented features	
JZ_{max}	Thickest part of the JZ, measured in the midsagittal and axial plane perpendicular to the endometrial cavity, in millimeters
JZ_{min}	Thinnest part of the visible JZ, measured in the midsagittal and axial plane perpendicular to the endometrial cavity, in millimeters
JZ_{diff}	JZ_{diff} is calculated as $JZ_{max\ (all\ planes)} - JZ_{min\ (all\ planes)}$, and represents irregularities of the JZ
$JZ_{max\text{-}A}$	JZ measurement including all low-intensity signal areas representing diffuse or circumscribed adenomyosis, attached to the JZ (see also Fig. 3)
Appearance of the JZ	Subjective impression of the JZ morphology being regular or irregular, not assessable or not visible (see Fig. 2).
JZ-to-myometrial thickness ratio	Using JZ_{max} in the midcorporal area (sagittal and axial) and the corresponding thickness of the myometrium obtained at the same measurement level. Only assessable when no fibroids distort the wall
Globular uterine shape	Subjective impression of the corpus uteri being round and caused by smooth muscular hypertrophy resulting in a globular uterine shape, not due to fibroids.
Number of fibroids	Fibroids, which appear as well-circumscribed uterine masses
Size of largest fibroid	Largest diameter (in millimeters)

[a] Primary outcome measure; *JZ*, junctional zone; *MRI*, magnetic resonance imaging; *T1W*, T1-weighted; *T2W*, T2-weighted

MRI experience) also assessed the main outcomes (JZ_{max}, JZ_{min}, JZ_{diff}, $JZ_{max\text{-}A}$, morphological JZ classification) in order to allow the evaluation of the inter-reader agreement of those signs. The readings were performed independently on two different image sets, blinded to the clinical, sonographic, and histopathological data.

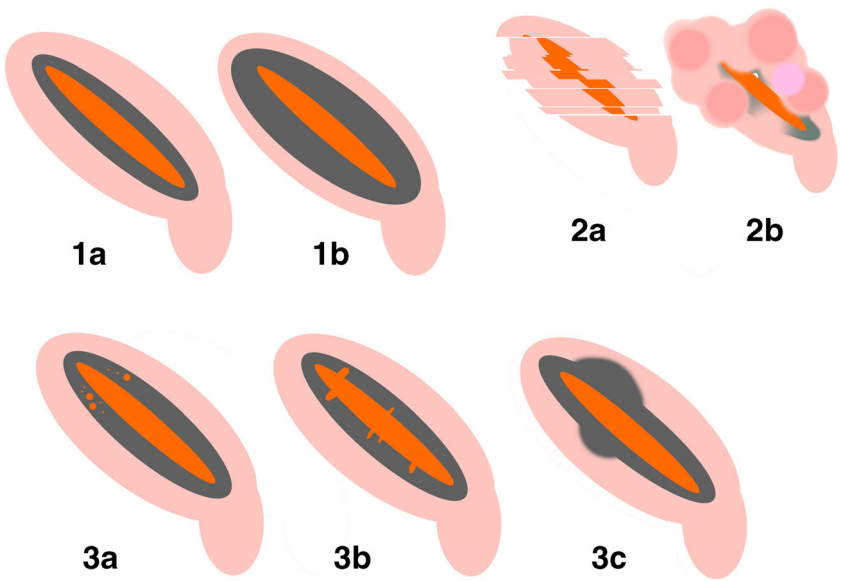

Fig. 2 Classification of the junctional zone (JZ) **1**: Regular JZ. The inner and outer borders of the JZ are linear and satisfyingly defined. (**1a**) thin JZ. (**1b**) regularly enlarged JZ. **2**: JZ not visible or not assessable. (**2a**) Due to motion artifacts. (**2b**) Due to fibroids or large areas of adenomyosis. **3**: Irregular, delineated JZ. If one or multiple of the following findings are present, and not caused by fibroids: (**3a**) JZ shows disruption by high-intensity foci (cysts), (**3b**) finger-like indentations at the endometrial-myometrial junction, and (**3c**) focal thickening of the JZ, not representing a contraction

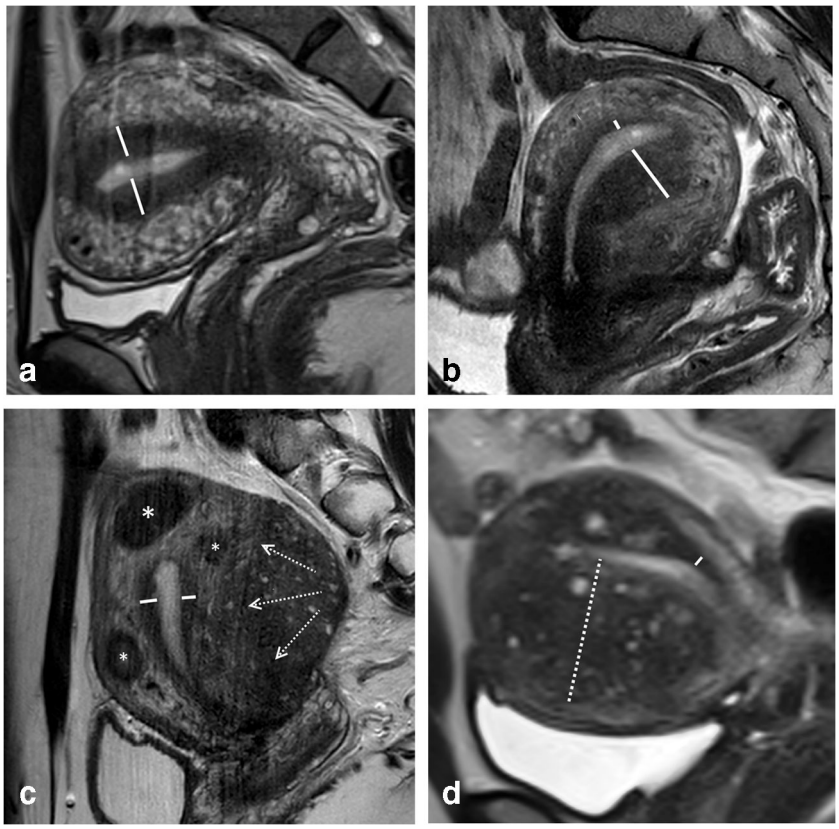

Fig. 3 Different methods used to define and measure the maximal thickness of the junctional zone (JZ). T2-weighted TSE MR images of the uterus. **a** The JZ is well defined and measured orthogonal to the cavity (line). **b** The JZ is enlarged in the posterior wall (JZ_{max}) and thin in the anterior wall (JZ_{min}). **c** Thin and visible JZ (line) and an area of adenomyosis growing toward the JZ (dotted arrows). Asterisk symbol indicates fibroids. **d** The JZ is only visible in the isthmic part of the posterior wall (line); the other parts are replaced by adenomyosis. We introduce the term "$JZ_{max\text{-}A}$" (dotted line) to discriminate this way of measuring from our definition of the JZ that does not include adenomyosis (**a**–**c**)

Reference standard

A positive outcome was defined as histopathologically confirmed adenomyosis. The pathological examination was performed in a standardized manner, cutting the fixated uterus in axial sections of 5–10-mm-thick slices. Microscopic sections were obtained based on instructions from the first investigator, covering areas of the hysterectomy specimen that appeared suspicious in the gross examination, where MRI had shown signs of adenomyosis, and/or randomly from at least every second slice in order to include all areas of the corpus [2]. The pathologist had no access to the imaging data. Two senior pathologists performed the microscopic histopathological analysis and made the final diagnosis. The presence of ectopic endometrial glands and stroma at 2.5 mm below the endometrial-myometrial junction was defined as adenomyosis [21].

Sample size and statistical analysis

The required sample size was derived based on the concept for range of confidence interval (CI) for specificity and sensitivity for the main predictor (maximum junctional zone thickness (JZ_{max}) ≥ 12 mm). Using a CI of 95% with a width of 0.2 and a test sensitivity and specificity of 75%, the nomogram showed that at least 73 study participants were required [22].

We used the Shapiro-Wilk test to test the normality of our samples. The proportions for categorical variables were compared with the chi-square test or Fisher's exact test. The sensitivity, specificity, accuracy, negative predictive value (NPV), and positive predictive value (PPV) were calculated. Numerical variables were analyzed using Student's *t* test or the Mann-Whitney *U* test. The receiver operating characteristics (ROC) curve and the area under the receiver operating characteristics curve (AUC) were used to identify linear variables that were significantly associated with the analyzed outcome. Multivariate linear regression was used to identify independent imaging predictors of adenomyosis. The simple pairwise Cohen κ statistic was used to measure the inter-reader agreement for categorical response imaging features, whereas the intraclass correlation coefficient (ICC) was used to assess the level of agreement for numerical response features. The κ and ICC values were categorized as follows: 0–0.20, slight agreement; 0.21–0.40, fair agreement; 0.41–0.60, moderate agreement; 0.61–0.80, substantial agreement; and 0.81–1, almost perfect agreement [23]. Statistical analysis was performed using IBM SPSS Statistics (version 25, IBM Corporation), and a probability value of $p \leq 0.05$ was considered statistically significant.

Table 3 Diagnostic performance of diagnostic predictors, reader 1

Predictor	Adenomyosis, $n = 57$ (%)	No adenomyosis, $n = 36$ (%)						p
Categorical variables			Sensitivity, (95% CI)	Specificity, (95% CI)	PPV, (95% CI)	NPV, (95% CI)	Accuracy, (95% CI)	
$JZ_{max} \geq 12$ mm	30 (53)	16 (50)	53% (39, 66%)	56% (38, 72%)	65% (55, 74%)	43% (33, 53%)	54% (43, 64%)	0.44
Presence of myometrial cysts	40 (70)	4 (11)	70% (57, 82%)	89% (74, 97%)	91% (80, 96%)	65% (55, 74%)	77% (68, 86%)	< 0.001
Presence of adenomyoma	18 (32)	2 (6)	32% (20, 45%)	94% (81, 99%)	90% (69, 97%)	47% (42, 51%)	56% (45, 66%)	< 0.001
$JZ_{diff} \geq 5.5$ mm (optimum cutoff)	30 (53)	9 (25)	53% (39, 66%)	75% (58, 88%)	77% (64, 86%)	50% (42, 58%)	61% (51, 71%)	0.01
Presence of irregular JZ[a]	42/56 [a] (74)	6/35 [a] (22)	74% (60, 85%)	83% (67, 94%)	88% (77, 94%)	67% (51, 80%)	77% (68, 86)	< 0.001
Regular JZ as negative predictive sign [b]	14 (26)	29 (81)	81% (64, 92%)	75% (62, 86%)	67% (56, 77%)	86% (76, 92%)	77% (68, 86%)	< 0.001
Cysts and/or fingerlike indentations in the JZ	22 (39)	2 (6)	39% (26, 52%)	94% (81, 99%)	92% (73, 98%)	49% (44, 55%)	60% (50, 70%)	< 0.001
JZ-to-wall-thickness ratio $\geq 50\%$[b]	24/39[a] (62)	15/28[a] (54)	42% (29, 56%)	58% (41, 75%)	50% (50, 72%)	39% (31, 48%)	48% (38, 60%)	0.51
Globular corpus uteri [b]	29/44[a] (66)	13/23[a] (57)	51% (37, 64%)	64% (46, 79%)	69% (57, 79%)	45% (36, 54%)	56% (45, 66%)	0.16
Numerical variables	Mean ± SD (mm)		p	AUC (95% CI)				p
JZ_{max} (mm)	11.1 ± 3.3	10.4 ± 3.9	0.37	0.57 (0.44, 0.70)				0.26
JZ_{diff} (mm)	8.4 ± 9.2	4.5 ± 3.1	0.02	0.62 (0.50, 0.74)				0.06
$JZ_{max\text{-}A}$ (mm)	15.8 ± 11.9	10.4 ± 3.9,	0.01	0.68 (0.57, 0.80)				< 0.001

Adenomyosis/no adenomyosis confirmed by histopathology. [a] n differs from the total if the feature was not assessable due to motion artifacts. [b] Not assessable cases (due to distortion of the uterine shape by fibroids) were counted as negative for this sign. *AUC*, area under the receiver operating characteristics curve; *CI*, confidence interval; *NPV*, negative predictive value; *PPV*, positive predictive value. *P* was determined using the chi-square test or Fisher's exact test; $p \leq 0.05$ was considered statistically significant

Table 4 Diagnostic performance of diagnostic predictors, reader 2

Predictor	Adenomyosis, $n = 57$ (%)	No adenomyosis, $n = 36$ (%)						*p*
Categorical variables			Sensitivity (95% CI)	Specificity (95% CI)	PPV (95% CI)	NPV (95% CI)	Accuracy (95% CI)	
$JZ_{max} \geq 12$ mm	30 (53)	16 (50)	53% (39, 66%)	56% (38,72%)	65% (55, 74%)	43% (33, 53%)	54% (43, 64%)	0.44
JZmax ≥ 12 mm	19 (33)	14 (39)	33% (21, 47%)	61% (44, 77%)	58% (44, 70%)	37% (30, 44%)	44% (34, 55%)	0.59
$JZ_{diff} \geq 6.5$ mm (optimum cutoff for R2)	28 (49)	7 (19)	49% (36, 63%)	81% (64, 92%)	80% (66, 89%)	50% (43, 58%)	62% (51, 71%)	0.01
Presence of irregular JZ	39/56 [a] (68)	6/35 [a] (22)	68% (56, 80%)	83% (67, 94%)	87% (75, 93%)	63% (53, 72%)	74% (64, 83%)	< 0.001
Regular JZ as negative predictive sign [b]	14 (26)	28 (78)	78% (61, 90%)	75% (62, 86%)	67% (55, 77%)	84% (74, 91%)	76% (66, 85%)	< 0.001
Presence of cysts in the JZ	16 (28)	1 (3)	33% (20, 47%)	97% (86, 100%)	94% (69, 99%)	52% (47, 57%)	60% (49, 71%)	< 0.001
Cysts and/or fingerlike indentations in the JZ	22 (39)	2 (6)	39% (26, 52%)	94% (81, 99%)	92% (73, 98%)	49% (44, 55%)	60% (50, 70%)	< 0.001
Numerical variables	Mean ± SD (mm)		*p*	AUC (95% CI)				*p*
JZ_{diff}	10.5 ± 12.4	5.2 ± 2.8	0.02	0.65 (0.53, 0.77)				0.06
JZ_{max}	10.3 ± 3.7	10.1 ± 3.7	0.85	0.50 (0.37, 0.62)				0.97
JZ_{max-A}	15.7 ± 12.6	10.3 ± 3.7	0.02	0.64 (0.53, 0.76)				0.02

Adenomyosis/no adenomyosis confirmed by histopathology. [a] *n* differs from the total if the feature was not assessable due to motion artifacts. [b] Not assessable cases (due to distortion of the uterine shape by fibroids) were counted as negative for this sign. *AUC*, area under the receiver operating characteristics curve; *CI*, confidence interval; *NPV*, negative predictive value; *PPV*, positive predictive value. *P* was determined using the chi-square test or Fisher's exact test; $p \leq 0.05$ was considered statistically significant

Results

$JZ_{max} \geq 12$ mm was not significantly associated with having adenomyosis, and the frequency of a $JZ_{max} \geq 12$ mm was similar in the groups with and without adenomyosis ($n = 30/57$ (53%) vs $n = 16/36$ (44%), $p = 0.29$). This was the case for both readers and each reading (individual results in Tables 3 and 4). Myometrial cysts and adenomyoma were the signs with the highest specificities; the detailed results of their diagnostic performance are listed in Table 3.

Combining the primary diagnostic markers $JZ_{max} \geq 12$ mm, myometrial cysts and adenomyoma, resulted in 41/57 (72%) true-positive, 12/36 (33%) false-positive, 19/36 (53%) true-negative, and 13/57 (23%) false-negative cases, and 8/93 (9%) cases being undetermined. The combined test quality when accounting for the undetermined cases as being respectively positive or negative could be quantified as follows (with 95% CI values in brackets): sensitivity of 77% (64, 87%) and 72% (59, 83%), specificity of 53% (36, 70%) and 67% (49, 81%), PPV of 72% (64, 79%) and 77% (68, 81%), NPV of 59% (45, 72%) and 60% (48, 70%), and accuracy of 68% (57, 77%) and 70% (60, 79%) (all $p < 0.001$).

The criterion of $JZ_{max} \geq 12$ mm was present in all false-positive cases and in 7/12 (58%) as the sole predictor. Figure 4 illustrates the examples of false-positive cases with $JZ_{max} \geq 12$ mm. In 3/12 (25%) of the false-positive cases, a single myometrial cyst was seen and interpreted as adenomyosis, and in 2/12 (17%) of the false-positive cases, fibroids with diffuse borders were interpreted as adenomyoma. Six of the seven false-negative cases (86%) showed $JZ_{max} < 12$ mm as a predictor. JZ_{max} was not correlated with the diagnosis of adenomyosis (AUC = 0.6; 95% CI, 0.48, 0.72; $p = 0.11$). JZ_{diff} showed an almost statistically significant association in this reading (AUC = 0.62; 95% CI, 0.50, 0.74; $p = 0.06$). With a cutoff of $JZ_{diff} \geq 5.5$ mm, a sensitivity of 53% and specificity of 75% were reached when using this as a categorical variable. We found a weak correlation with a positive outcome for the $JZ_{max\text{-}A}$ and adenomyosis (AUC = 0.68; 95% CI = 0.57, 0.80; $p < 0.001$). The JZ-to-myometrial thickness ratio was not statistically significant associated with adenomyosis (AUC =

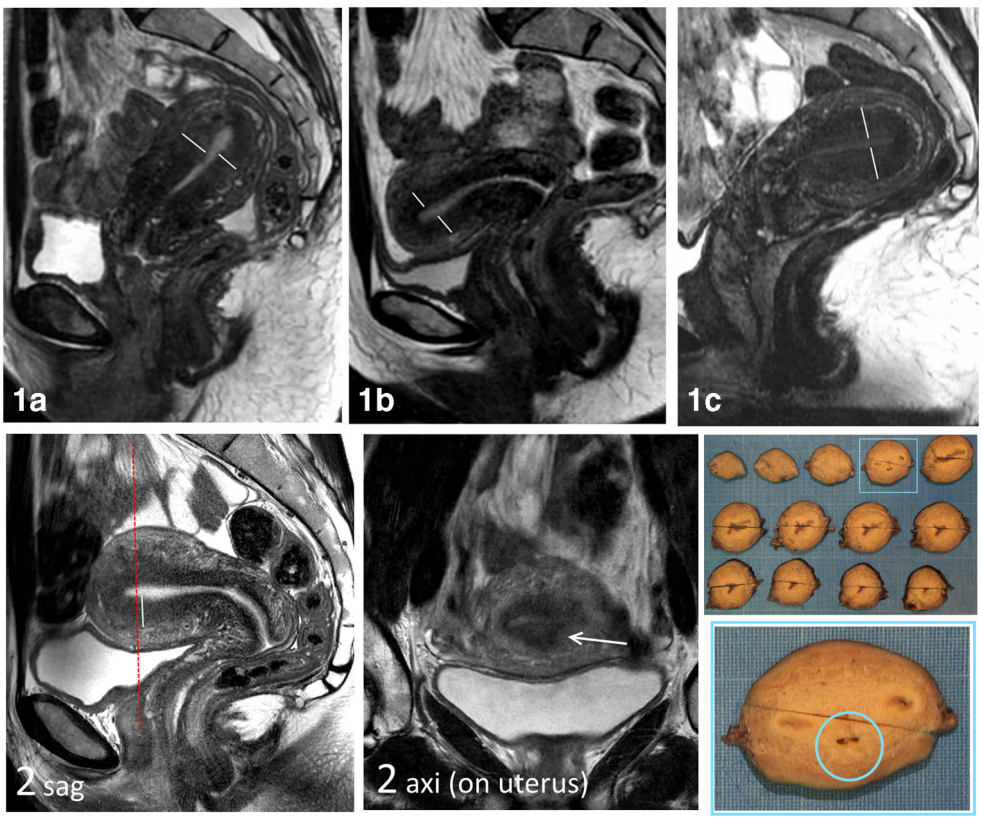

Fig. 4 False-positive and false-negative cases with a regular junctional zone (JZ) and JZ thickness ≥ 12 mm. T2-weighted TSE MR images of the uterus. The presence of adenomyosis was determined by histopathology. **Cases 1A–C** are false-positive when using a cutoff of JZ ≥ 12 mm as diagnostic marker, but true-negative with pattern recognition of the JZ morphology (regular JZ). **Case 2** (all images below), JZ 12 mm. The JZ was falsely classified as regular because the irregularity in the true axial plane of the uterus was misinterpreted as a uterine contraction (image cross-reference is indicated with the red, stippled line in the sagittal plane of the uterus, where the focal thickening is not visible). Histopathology showed adenomyosis in that area, visible in the gross examination, illustrated on the lower-right pictures. A 5-7-mm-thick axial sections of the formalin-fixed hysterectomy specimen, slice 4 (blue box, enlarged below), contained a focus of adenomyosis (blue ring) that corresponds to the irregularity of the JZ as seen on the true axial image in MRI

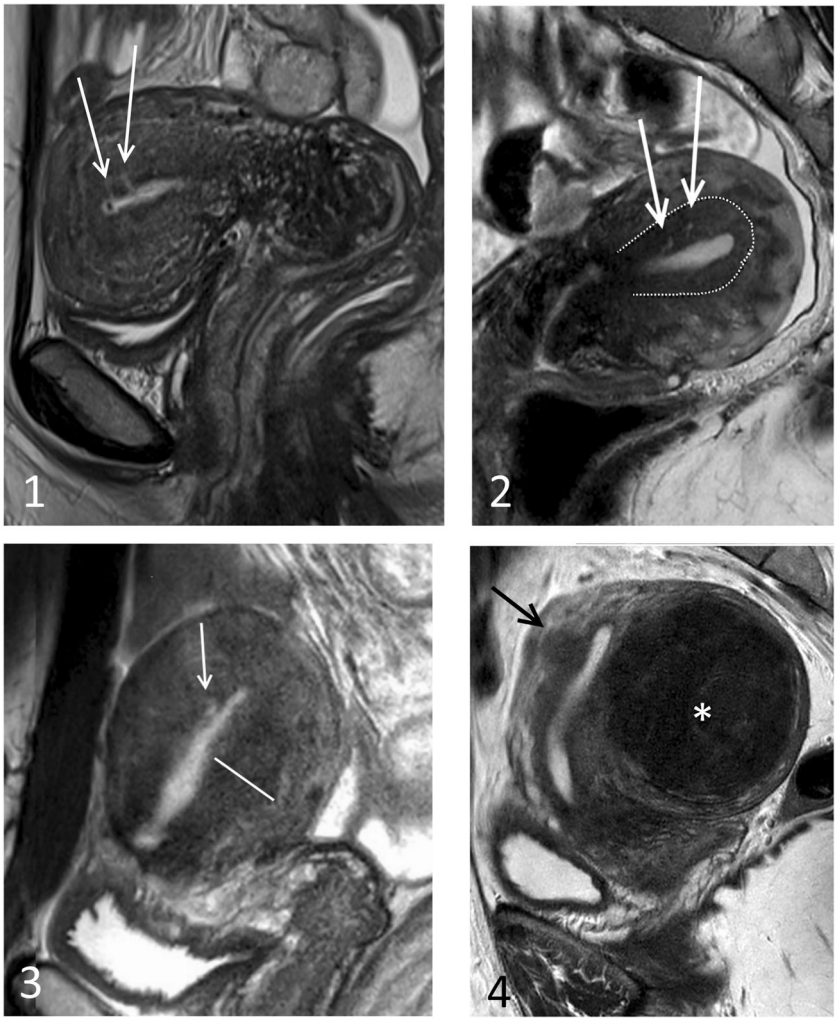

Fig. 5 Cases with an irregular junctional zone (JZ), true-positive and false-positive. T2-weighted TSE MR images of the uterus, all in sagittal plane. The presence of adenomyosis was determined by histopathology. **1**: The JZ is not visible in the fundus and thin (max. 6mm) in the visible parts. Finger-like invasion of adenomyosis to the myometrium (arrows) visible. True positive diagnosis **2**: High-intensity signals on the inner border (arrows) representing infiltration of adenomyosis that interrupts the JZ. The outer border of the JZ (stippled line) should not be confused with the low-intensity signal from the stratum vasculare. True-positive diagnosis. **3**: The JZ (line) is thickened (14mm) in the posterior wall and thin in the anterior wall, where also a high-signal focus can be seen (arrow). True positive diagnosis **4**: Uterus with a large fibroid in the posterior wall (marked with an asterisk). Focal thickening to 14 mm of the JZ in the anterior wall (arrow) represented a small fibroid but was falsely classified as JZ irregularity due to its diffuse demarcation. False-positive diagnosis

0.54; 95% CI, 0.40, 0.69%; $p = 0.54$). The diagnostic performance of the other documented features is presented in Table 3, and the number and size of fibroids are presented in Table 1.

JZ morphology

The presence of an interrupted and/or irregular JZ was strongly correlated with having adenomyosis, while a regular JZ was strongly correlated with not having adenomyosis (both $p < 0.001$, detailed diagnostic performance in Table 3). Figure 2 illustrates the categories of JZ, while Figs. 4 and 5 depict MR images of regular and irregular JZ. The JZ was sufficiently well depicted in 91/93 (98%) of cases; in the remaining 2 cases, it was not assessable due to motion artifacts.

In the multiple linear regression analysis, only the presence of an irregular JZ ($\beta = 0.16$, $p = 0.006$) and myometrial cysts ($\beta = 0.18$, $p = 0.005$) showed an independent association with having adenomyosis. The choice of MRI system did not influence the results.

Intra- and inter-reader agreement

There was a substantial intra-reader agreement in the measured JZ_{max} values (first and second readings performed by R1), with an ICC of 0.75 (95% CI, 0.59, 0.84; $p < 0.001$). The inter-reader agreements were almost perfect for the measured values of JZ_{max} (ICC = 0.81; 95% CI, 0.70, 0.87; $p < 0.001$) and $JZ_{max\text{-}A}$ (ICC = 0.95; 95% CI, 0.93, 0.97; $p < 0.001$), and substantial for JZ_{diff} (ICC = 0.73; 95% CI, 0.59, 0.83; $p < 0.001$). The inter-reader agreement for the classification of the JZ was almost perfect ($\kappa = 0.89$; 95% CI, 0.78, 0.97).

Discussion

In this prospective, single-center study, adenomyosis was not correlated with JZ_{max} or the previously proposed JZ_{max} cutoff of 12 mm, which is contrary to previously published prospective studies [9–11]. A diagnose of adenomyosis based on these JZ measurements contributed to a high number of false-positive and false-negative diagnoses in our study population.

There are several possible explanations for why our results differ from those of previous studies. Firstly, the mean age of our study participants was lower (42 years vs 51 years), and it is known that adenomyosis progresses over time and hence could have been more extensive in the previous studies. Secondly, Reinhold and Bazot also included a large proportion of postmenopausal women in their study (31–55%), and it is questionable whether diagnostic characteristics of the hormone-dependent JZ are transferable between pre- and postmenopausal populations [9, 11].

Thirdly, we measured the JZ in accordance with our usual clinical practices, since there is neither a unanimous classification of adenomyosis nor a clear definition of the JZ; the main reason for that is most likely that the JZ has the same signal intensity as adenomyosis and that it is not visible in histopathology [7, 24]. It is not ultimately clear how the JZ was defined in other studies.

We find using JZ thickness measurements that included all low-intensity areas, also those representing diffuse or circumscribed adenomyosis that are in connection with the JZ ($JZ_{max\text{-}A}$) problematic for several reasons. In those cases, the presence of adenomyosis is usually obvious and therefore performing a measurement does not add any diagnostic value. If $JZ_{max\text{-}A}$ is measured in a study population with extensive disease, a statistically significant association with adenomyosis is likely to be found. However, this association might not be equally meaningful for individual evaluation and in clinical practice, especially not in younger women of childbearing age and less extensive disease [25]. The interest in adenomyosis has shifted toward younger, infertile women and defining dedicated diagnostic markers for this group is of great importance. Bazot and Darai have recently stated that "In our experience, the JZ_{max} alone should be used with caution to diagnose internal adenomyosis." This is in line with the conclusion of all the authors of comparable studies, who all state that other signs in addition to JZ measurements have to be considered [7, 9–11].

We introduce a classification of the JZ that reflects different kinds of JZ irregularities based on pattern recognition. This classification showed an almost perfect inter-reader agreement. Combined with signs of adenomyosis of the outer myometrium (adenomyoma and myometrial cysts), we yielded a sensitivity of 81% and specificity of 81%, which are comparable to the performance of various combined markers in previous studies with sensitivities of 86%, 77%, and 64% and specificities of 86%, 93%, and 88% [9–11]. The sensitivity in our study was higher than in two of the others, probably because our MR images were obtained from thinner slices (1 to 3 mm thick, with a gap of 0.5 to 0.3 mm, vs 4 mm and a gap of 2 mm).

Our study was subject to some limitations. The post hoc decision for the second read might have influenced the results of the second reading, though a high intra- and inter-reader correlation shows the consistency of the readings. Like all studies involving hysterectomy with histopathology as the gold standard in diagnosing adenomyosis as an outcome, a selection bias is likely to have been present. Women that undergo hysterectomy might have more-severe disease and possibly different phenotypes of adenomyosis than women receiving conservative treatment. Furthermore, the MRI images were obtained during random phases of the menstrual cycle. There is conflicting evidence on the extent to which this is relevant, but it might have affected the measurements [7, 26]. Also, we did not exclude cases due to a certain time interval between MRI and surgery. One might argue that the progression of the disease might influence the results, but that would result in false-negative cases among those with a long time gap between imaging and surgery. In our data, the false-negative cases all show a time interval of under 3 months, with one exception, where a well-circumscribed adenomyoma was interpreted as a fibroid. As this study does not quantify the amount of adenomyosis found, we consider also longer time gaps as acceptable.

One major strength of our study is the performing of very thorough histopathological examinations, which aimed at achieving a high diagnostic sensitivity and also most likely resulted in the prevalence of adenomyosis being much higher (61%) than in other studies (21–33%). The clinical implications of very small adenomyosis, foci that might be detected only by a thorough histological, is not clear. However, in a study of diagnostic accuracy like the present, we think that a very thorough diagnosis is imperative and the clinical relevance of small findings needs to be determined in other studies. Another strength is that we used two independent readers who exhibited extremely high inter-reader agreement. Furthermore, we did not exclude patients with fibroids, since fibroids often coexist with adenomyosis and the exclusion might lead to an exaggeration of diagnostic performance of some predictors.

Conclusions

The irregular appearance of the junctional zone and the presence of myometrial cysts are independent predictors of adenomyosis. Measurements of the JZ had no statistically significant association with the presence of adenomyosis in our study population. JZ measurements are not validated for a young patient population with moderate disease and should therefore be used with caution.

Acknowledgments The authors thank Else Kathrine Skovholt, M.D. for the analysis of the histopathological specimen.

Funding The first author received a PhD-grant from the Norwegian Women's Health Association (Norske Kvinners Sanitetsforening) to

perform this study (grant number NKS14901), who was involved in neither the design, data analysis, nor publication of this study.

Compliance with ethical standards

Guarantor The scientific guarantor of this publication is Prof. Marit Lieng.

Conflict of interest The authors of this manuscript declare no relationships with any companies whose products or services may be related to the subject matter of the article.

Statistics and biometry Staale Nygaard kindly provided statistical advice for this manuscript. Also, several of the authors have significant statistical expertise. However, no complex statistical methods were necessary for this paper.

Informed consent Written informed consent was obtained from all subjects in this study.

Ethical approval Institutional Review Board approval was obtained.

Study subjects or cohorts overlap Ultrasound examination was performed on the whole study cohort; the results are reported elsewhere [12]. The data reported in this article have no overlap with previously published work.

Methodology
- Prospective
- Diagnostic or prognostic study
- Performed at one institution

References

1. Naftalin J, Hoo W, Pateman K, Mavrelos D, Holland T, Jurkovic D (2012) How common is adenomyosis? A prospective study of prevalence using transvaginal ultrasound in a gynaecology clinic. Hum Reprod 27:3432–3439
2. Bird CC, McElin TW, Manalo-Estrella P (1972) The elusive adenomyosis of the uterus–revisited. Am J Obstet Gynecol 112: 583–593
3. Choi EJ, Cho SB, Lee SR et al (2017) Comorbidity of gynecological and non-gynecological diseases with adenomyosis and endometriosis. Obstet Gynecol Sci 60:579–586
4. Li X, Liu X, Guo SW (2014) Clinical profiles of 710 premenopausal women with adenomyosis who underwent hysterectomy. J Obstet Gynaecol Res 40:485–494
5. Younes G, Tulandi T (2017) Effects of adenomyosis on in vitro fertilization treatment outcomes: a meta-analysis. Fertil Steril 108: 483–490 e483
6. Bruun MR, Arendt LH, Forman A, Ramlau-Hansen CH (2018) Endometriosis and adenomyosis are associated with increased risk of preterm delivery and a small-for-gestational-age child: a systematic review and meta-analysis. Acta Obstet Gynecol Scand 97: 1073–1090
7. Bazot M, Darai E (2018) Role of transvaginal sonography and magnetic resonance imaging in the diagnosis of uterine adenomyosis. Fertil Steril 109:389–397
8. Agostinho L, Cruz R, Osorio F, Alves J, Setubal A, Guerra A (2017) MRI for adenomyosis: a pictorial review. Insights Imaging 8:549–556
9. Reinhold C, McCarthy S, Bret PM et al (1996) Diffuse adenomyosis: comparison of endovaginal US and MR imaging with histopathologic correlation. Radiology 199:151–158
10. Dueholm M, Lundorf E, Hansen ES, Sorensen JS, Ledertoug S, Olesen F (2001) Magnetic resonance imaging and transvaginal ultrasonography for the diagnosis of adenomyosis. Fertil Steril 76: 588–594
11. Bazot M, Cortez A, Darai E et al (2001) Ultrasonography compared with magnetic resonance imaging for the diagnosis of adenomyosis: correlation with histopathology. Hum Reprod 16:2427–2433
12. Tellum T, Nygaard S, Skovholt EK, Qvigstad E, Lieng M (2018) Development of a clinical prediction model for diagnosing adenomyosis. Fertil Steril 110:957–964
13. Byun JY, Kim SE, Choi BG, Ko GY, Jung SE, Choi KH (1999) Diffuse and focal adenomyosis: MR imaging findings. Radiographics 19 Spec No:S161–S170
14. Tamai K, Togashi K, Ito T, Morisawa N, Fujiwara T, Koyama T (2005) MR imaging findings of adenomyosis: correlation with histopathologic features and diagnostic pitfalls. Radiographics 25:21–40
15. Togashi K, Nishimura K, Itoh K et al (1988) Adenomyosis: diagnosis with MR imaging. Radiology 166:111–114
16. Togashi K, Ozasa H, Konishi I et al (1989) Enlarged uterus: differentiation between adenomyosis and leiomyoma with MR imaging. Radiology 171:531–534
17. Stamatopoulos CP, Mikos T, Grimbizis GF et al (2012) Value of magnetic resonance imaging in diagnosis of adenomyosis and myomas of the uterus. J Minim Invasive Gynecol 19:620–626
18. Van den Bosch T, Dueholm M, Leone FP et al (2015) Terms, definitions and measurements to describe sonographic features of myometrium and uterine masses: a consensus opinion from the Morphological Uterus Sonographic Assessment (MUSA) group. Ultrasound Obstet Gynecol 46:284–298
19. Novellas S, Chassang M, Delotte J et al (2011) MRI characteristics of the uterine junctional zone: from normal to the diagnosis of adenomyosis. AJR Am J Roentgenol 196:1206–1213
20. Tamai K, Koyama T, Umeoka S, Saga T, Fujii S, Togashi K (2006) Spectrum of MR features in adenomyosis. Best Pract Res Clin Obstet Gynaecol 20:583–602
21. Bergeron C, Amant F, Ferenczy A (2006) Pathology and physiopathology of adenomyosis. Best Pract Res Clin Obstet Gynaecol 20: 511–521
22. Machin D, Campbell MJ, Tan SB, Tan SH (2008) Sample size tables for clinical studies, 3rd edn. Wiley-Blackwell, Oxford
23. Watson PF, Petrie A (2010) Method agreement analysis: a review of correct methodology. Theriogenology 73:1167–1179
24. Mehasseb MK, Bell SC, Brown L, Pringle JH, Habiba M (2011) Phenotypic characterisation of the inner and outer myometrium in normal and adenomyotic uteri. Gynecol Obstet Invest 71:217–224
25. Halligan S, Altman DG, Mallett S (2015) Disadvantages of using the area under the receiver operating characteristic curve to assess imaging tests: a discussion and proposal for an alternative approach. Eur Radiol 25:932–939
26. Kang S, Turner DA, Foster GS, Rapoport MI, Spencer SA, Wang JZ (1996) Adenomyosis: specificity of 5 mm as the maximum normal uterine junctional zone thickness in MR images. AJR Am J Roentgenol 166:1145–1150